ELSEVIER

Journal of Chromatography A, 911 (2001) 27–37

JOURNAL OF CHROMATOGRAPHY A

www.elsevier.com/locate/chroma

Quantitative interpretation of Fourier-transform infrared spectroscopic data from a size-exclusion chromatography solvent–evaporation interface

Askar Karami[a], Stephen T. Balke[a], Timothy C. Schunk[b,*]

[a]*Department of Chemical Engineering and Applied Chemistry, University of Toronto, Toronto, Ontario, Canada*
[b]*Imaging Materials and Media — Research and Development, Eastman Kodak Company, Kodak Park, Building 82, Rochester, NY 14650-2136, USA*

Received 10 August 2000; received in revised form 31 October 2000; accepted 21 November 2000

Abstract

Quantitative evaluation of polymer composition across the SEC chromatogram can provide more accurate characterization of heterogeneous polymer samples for problem solving and for material specification. To this end Fourier-transform infrared spectroscopy (FTIR) with solvent–evaporation interfaces has become a very powerful detector for size-exclusion chromatography (SEC). The solvent–evaporation interface removes the mobile phase at the exit of the chromatograph and deposits the separated molecular sizes as polymer films on infrared transparent substrates. Quantitative interpretation of the FTIR spectra obtained from these films has recently been found to be best accomplished by using partial least squares. In this paper, polystyrene and poly(methylmethacrylate), alone, as blends, and a copolymer were analyzed in a SEC equipped with an evaporative interface. Molecular weight effects, wavelength selection, the effect of averaging spectra on results, and selection of the best data preprocessing method were investigated. General methods of evaluating these variables were developed to arrive at conditions for this particular ''model'' situation in order to provide a basis for the analysis of more complex polymers.

Keywords: Fourier-transform infrared spectroscopy; Detection, LC; Solvent–evaporation interface; Partial least squares; Polymers; Polystyrene; Poly(methylmethacrylate)

1. Introduction

Fourier-transform infrared spectroscopy (FTIR) is potentially a very powerful detector for size-exclusion chromatography (SEC). The main obstacle to its use has been the interfering absorbance of the SEC mobile phase. In recent years, solvent–evaporation interfaces have begun to be used to remove the mobile phase at the exit of the chromatograph. The separated molecular sizes can be collected as a series of polymer films on infrared transparent substrates either on separate disks [1–4], or as a deposited stripe of polymer on a moving substrate [5–7]. Our research has employed two solvent–evaporation interfaces, both utilizing separate disks, and revealed that polymer film quality generated by the interface was of critical importance to quantitative interpretation of the data [2–4,7–10]. Distorted spectra and inconsistent values even from apparently normal

*Corresponding author. Tel.: +1-716-722-9508.
E-mail address: timothy.schunk@kodak.com (T.C. Schunk).

0021-9673/01/$ – see front matter
PII: S0021-9673(00)01186-9

spectra were readily obtained because of bare spots or other non-uniformities in the films. The main outcome of this previous work was a method of annealing the films after they were deposited by exposing them to solvent vapors. Once quality films are obtained, the issues then centered on how to best obtain valid concentration values from the spectra. A primary concern is analysis of polymer blends and copolymers. In our most recent publication [3,4] we examined many alternative computational methods that can be applied to the data and concluded that a multi-variate method, partial least squares (PLS) applied to the second derivative of absorbance with respect to wavelength, provided the best results. Also, although PLS was shown to be capable of providing attractive blend composition values when used with either annealed or ''as-collected'' films, the latter data showed high error when total mass injected was calculated. Thus, solvent annealing was considered necessary to ensure reliable results even when PLS was employed. Other research groups have focused on the use of classical linear regression of band area ratio data to address polymer composition distributions with solvent–evaporation interface FTIR data [11–13]. Limited evaluation of accuracy and precision has been discussed and in some cases [13] uncalibrated data has been presented.

In this paper, building upon our previous results, we focus upon the use of PLS in the quantitative analysis of data on polymer blends and copolymers obtained using the solvent–evaporation interface. As with our prior work, we present procedures for the critical evaluation of quantitative results using data obtained from an FTIR solvent–evaporation interface by using examples of well-defined systems [3,4]. Molecular weight effects, wavelength selection, the effect of spectral averaging on results, and selection of the best data preprocessing method were investigated.

2. Theory

2.1. Quantitative measures of precision and accuracy

In this work, the ''true'' value for determination of accuracy is considered as that mass of polymer on the disk as estimated from the differential refractive index chromatogram. The precision measures used in this work include residuals (R_j), root mean square error of calibration (RMSEC), root mean square error of prediction (RMSEP), and relative error (RE). These are described in turn below.

A residual, R_j, is defined in terms of percentage error by:

$$R_j = 100\frac{w_{j,FTIR} - w_{j,DRI}}{w_{j,DRI}} \tag{1}$$

where w_j is the weight fraction of one of the components present from the jth sample where the method used to measure w_j is indicated by the subscript FTIR or differential refractive index (DRI). R_j can be plotted against $w_{j,DRI}$. In this case scatter of the residuals show precision and the proximity of the values to zero show accuracy.

RMSEC is defined by:

$$RMSEC = \sqrt{\frac{\sum_{j=1}^{n}(w_{j,DRI} - w_{j,FTIR})^2}{n}} \tag{2}$$

where n is the number of SEC–evaporative interface runs used in calibration. Therefore, RMSEC is a measure of how well the composition values obtained from the calibration step of the FTIR interpretation match the ''true'' values.

RMSEP is very similar to RMSEC except it is applied to data not used in the calibration:

$$RMSEP = \sqrt{\frac{\sum_{j=1}^{m}(w_{j,DRI} - w_{j,FTIR})^2}{m}} \tag{3}$$

where m is the number of SEC–evaporative interface runs not used for calibration. RMSEP is thus a measure of the prediction ability of the analysis.

Relative error (RE) is defined by:

$$RE = 100\left(\frac{\sum_{i=1}^{k} m_{i,FTIR} - \sum_{i=1}^{k} m_{i,DRI}}{\sum_{i=1}^{k} m_{i,DRI}}\right) \tag{4}$$

where m_i is the mass of fraction i as determined by the indicated method (DRI or FTIR) and summed over k fractions collected across the SEC chromatogram.

2.2. Partial least squares

PLS characterizes the changes amongst spectra and concentration data from a ''calibration'' set [14]. The calibration spectra are represented as the matrix vector product of the full spectrum vectors (loading vectors) and the intensities (scores) plus a residuals matrix. The spectral intensities are then related to the concentrations by an inverse least-squares model. In building the PLS model it is important to select a sufficient number of factors (scores) so that a good fit can be obtained and good predictions made. However, if too many factors are selected then prediction ability will be impaired by fitting noise. A widely used method for estimating the correct number of factors is a cross-validation method obtained by sequentially leaving out one calibration spectrum at a time to calculate the prediction residual error sum of squares (*PRESS*):

$$PRESS = \sum_{j=1}^{n}\sum_{i=1}^{k}(m_{i,j,FTIR} - m_{i,j,DRI})^2 \quad (5)$$

where $m_{i,j,FTIR}$ is the mass of component i from sample j deposited on the disk and obtained from PLS. $m_{i,j,DRI}$ is the mass of component i from sample j deposited on the disk and obtained from the slice area on the DRI chromatogram. The optimum number of factors for a PLS model is determined as the least number providing a minimum *PRESS* value. In all cases for the work presented here, two or three factors were found to be optimal.

PLS consists of both a calibration and a prediction step. In this work there are two main types of sample data that can be used for the calibration: homopolymer data and polymer blend data. The main objective is to obtain a calibration that is suitable for copolymer analysis. In addition to the different types of data that can be used for the calibration there are a variety of ''practical'' issues to be resolved in applying PLS to the data. These are discussed in the following sections.

2.3. Screening peaks for molecular mass effects

Molecular weight affects viscosity of the eluent and hence possibly nebulization in the interface. This in turn can affect the quantity of the polymer captured by the germanium disks beneath the interface nozzle and the film quality. This effect was examined by injection of a series of narrow molecular mass distribution standards and investigation of how the area under the peak varied with molecular mass of the standards. The area used in this work is the area of the second derivative of the absorbance with respect to wavelength of an IR band. Calculation of the second derivative removes baseline displacement and linear baseline drift from the original spectrum.

2.4. Selecting candidate wavelengths for quantitative analysis

Table 1 shows the candidate wavelengths for the PS/PMMA blends and copolymers used in this work. There is some question as to whether PS absorbances at 537 cm^{-1} and 699 cm^{-1} would be unaffected by the presence of PMMA in the polymer film. That is, absorbances at these wavelengths need to be examined to see if they provide the same measure of styrene concentration regardless of whether or not PMMA was present in the sample. This can be done by examining the ratio of absorbances at these wavelengths to the absorbance at 1599 cm^{-1} as a function of PMMA concentration in PS/PMMA blends.

2.5. Averaging spectra

Averaging spectra is a well-known method of reducing noise in the data: the standard deviation of the individual absorbance values is expected to be reduced by a factor of $1/\sqrt{m}$, where m is the number of replicate scans. FTIR is normally run to provide average spectra. When used with an evaporative interface the main source of error is the variation

Table 1
PLS training set spectral regions

Spectral Range (cm^{-1})	Component
3066–2804	PMMA
1782–1681	PMMA
1639–1535	PS
1520–1378	PMMA
1056–983	PS
740–663	PS
582–500	PS

in each samples' spectrum from SEC run to run. Thus, in this study the spectra from replicate runs on the evaporative interface were averaged. The second derivative of the average spectra can then be used as inputs to PLS and the results examined.

2.6. Other data pre-processing methods

In addition to averaging, several pre-processing methods (methods applied before PLS is used) are available. These methods can be used alone or in various combinations. The three of interest here are: mean centering, multiplicative scatter correction, and standard normal variate.

Mean centering simply refers to subtracting the mean value of all $m_{i,j,DRI}$ from each of the individual values. A similar procedure is carried out with the absorbance spectra. This effectively removes variation in the mean value as one of the sources of variation in the mass values and in the spectra. This is one less source of variation to be accounted for when PLS is applied.

Multiplicative scatter correction (MSC) [15] is used to attempt to remove the effects of light scattering from the spectra. It is assumed that the absorbance values of a sample when plotted versus those of the mean of all spectra will fall upon a straight line that can be fit by simple linear regression. Each spectrum can then be ''corrected'' for scattering effects by using the slope and intercept of this line with the individual absorbance values. The method can be applied to absorbances or to the second derivative of absorbance with respect to wavelength as was done here.

Standard Normal Variate (SNV) [16] is another method of attempting to correct for scattering effects on the spectra. Each spectrum is normalized by the standard deviation of the responses across the entire wavelength range.

3. Experimental

3.1. Materials

Polystyrene (PS) NBS 706 was obtained from NIST (Washington, DC, USA) and poly(methylmethacrylate) (PMMA) broad standard lot 037B was obtained from Scientific Polymer Products (SP2) (Ontario, NY, USA). Narrow molecular mass distribution PS standards were obtained from American Polymer Standards (Mentor, OH, USA). Poly(styrene-co-methylmethacrylate) (SMM) random copolymer Cat# 15783 was obtained from Polysciences, (Warrington, PA, USA). Bulk copolymer composition was verified by C13-NMR.

3.2. Size-exclusion chromatography

SEC separations were performed on a three-column set of PLgel 10 μm 300×7.5 mm mixed bed columns (Polymer Laboratories, Amherst, MA, USA). A Waters 590 pump (Waters Associates, Milford, MA, USA) was used to deliver 1.0 ml/min of freshly distilled helium sparged tetrahydrofuran (THF). HPLC grade THF (J. T. Baker, Phillipsburg, NJ, USA) was distilled from calcium hydride (Eastman Kodak Company, Rochester, NY, USA) to eliminate peroxides and water. Polymer samples at 5.00 mg/ml total concentration in THF were injected from a 100 μl loop using a Rheodyne (Cotati, CA, USA) injection valve. All samples were analyzed at least in triplicate. A second Rheodyne valve was used to switch the solvent flow after the columns to either a Waters Model R401 differential refractive index (DRI) detector or the solvent–evaporation interface as shown in Ref. [3,4]. The solvent flow path was configured to provide equal volume from the switching valve to either the DRI or solvent–evaporation interface.

3.3. Solvent–evaporation interface

The results described in this work were generated using a custom built solvent–evaporation interface similar in basic design to that described by Dekmezian et al. [1]. A diagram of the solvent–evaporation interface is shown in Fig. 1. The interface consisted of a stainless steel temperature-controlled vacuum chamber. The temperature of the evaporation chamber was controlled by circulating silicone oil at 60°C with a Haake Model DC5-GH (Paramus, NJ, USA) circulating bath through the double walled chamber. During sample collection the chamber pressure was maintained at 25 Torr using a dry ice trapped vacuum pump to remove solvent vapor and a

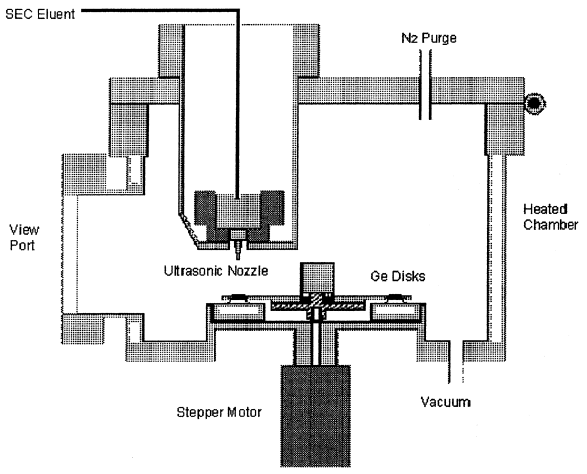

Fig. 1. Schematic diagram of the solvent–evaporation interface.

4.5 l/min N_2 purge. The stainless steel sample collection wheel was 150 mm in diameter with 20 equally spaced wells holding 13×2 mm polished germanium (Ge) disks (Spectral Systems, Hopewell Junction, NY, USA) as collection substrates. The collection wheel was maintained at 90°C on a nickel-plated copper stage temperature controlled with silicone oil from a Haake Model A81 circulating bath. The SEC solvent stream was sprayed onto the Ge disks using a Sonotek (Poughkeepsie, NY, USA) 120 kHz ultrasonic nozzle at 0.50 W power. The nozzle temperature was stabilized at 30°C with a 40 psig N_2 stream inside the nozzle housing.

For each SEC analysis the interface chamber was equilibrated with the THF vapor of the SEC eluent after sample injection prior to the start of polymer elution. SEC samples were collected as 19 fractions, each of equal duration depending upon the breadth of the SEC peak, across the SEC chromatogram by positioning the sample wheel with a computer controlled Slo-Syn stepper motor (Superior Electric, Bristol, CT, USA).

3.4. Sample preparation and FTIR analysis

After sample collection, a cover plate was placed over the sample wheel and the assembly removed from the collection chamber. To improve collected film uniformity and minimize IR scattering distortions, each Ge disk was briefly exposed to the vapor above refluxing dichloromethane (J.T. Baker) after the sample wheel was removed from the interface. After this solvent annealing, the sample wheel was placed on a similar stepper motor drive in the FTIR spectrometer. FTIR spectra were obtained at 8 cm^{-1} resolution with 32 coaveraged scans using Mattson WinFirst software. Spectra were obtained with a Mattson Polaris Spectrometer (Madison, WI, USA).

3.5. Data analysis

Spectral peak fitting was performed using PeakFit software (SPSS, Chicago, IL, USA). Second derivatives of the IR absorbance spectra were determined numerically using a Savitsky–Golay algorithm (SG2) with a second-degree five point smooth. Band area of each second derivative IR spectrum was determined as the baseline corrected area under the central peak of the second derivative after multiplication of each height of the second derivative chromatogram by negative one. PLS calibration models and quantitative calculations were performed using PLS IQ GRAMS/32 software (Galactic Industries, Salem, New Hampshire, USA).

4. Results and discussion

4.1. Screening peaks for molecular mass effects

Because polymer molecular mass can affect nebulization in the interface it can influence both the efficiency of collection of the sample on the germanium disks and the quality of the resulting film. To examine this effect, several samples of very narrow molecular mass distribution polystyrenes with peak molecular masses ranging from 1.4×10^3 to 1.6×10^6 g/mol were analyzed at constant injected concentration using the interface. Results are shown in Fig. 2 as a plot of the area under the spectral peak at 699 cm^{-1} versus the molecular mass of the polystyrene analyzed. Results from both peak fitting of the conventional spectra [3,4] and those obtained from the area under the valley portion of the second derivative spectra (see description in the experimental section) demonstrated a constant area only at molecular masses above 200 000. Below 200 000, the area under the 699 cm^{-1} peak decreases. It was

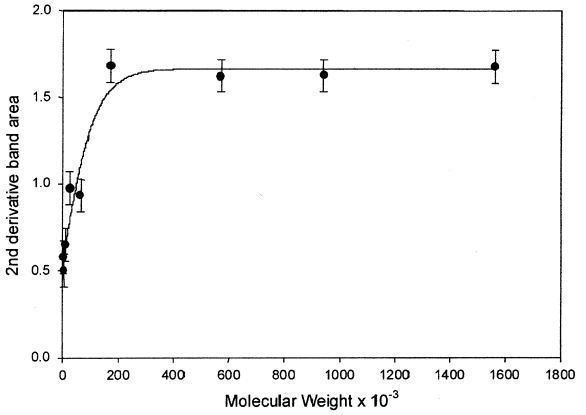

Fig. 2. Effect of molecular mass of narrow molecular mass distribution PS standards on the area under $d^2A/d\lambda^2$ at 699 cm^{-1}.

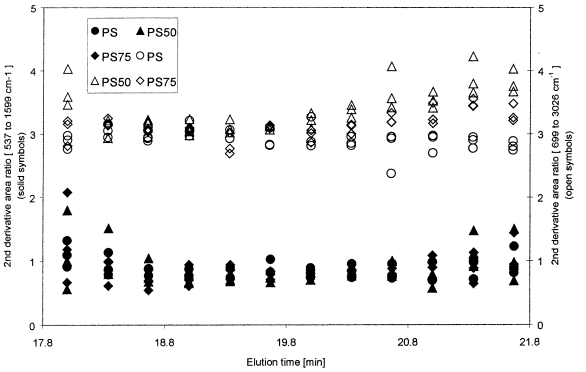

Fig. 3. Test for the effect of the presence of PMMA on absorbances used for polystyrene analysis: (a) ratio of area under $d^2A/d\lambda^2$ at 537 cm^{-1} to the area under $d^2A/d\lambda^2$ at 1599 cm^{-1} versus elution time and (b) ratio of area under $d^2A/d\lambda^2$ at 699 cm^{-1} to the area under $d^2A/d\lambda^2$ at 3026 cm^{-1} versus elution time, for three samples: PS, polystyrene alone; PS50, a 50:50 by wt. blend of PS and PMMA; PS75, a 75:25 by wt. blend of PS and PMMA.

hypothesized that this result was due to lower particle collection efficiencies by the germanium disks for lower-molecular-mass polymers. The lower viscosities associated with these molecular masses are expected to result in smaller droplets formed by the ultrasonic nozzle [17,18]. These smaller droplets then would become smaller particles and be more readily swept from the chamber by the flowing nitrogen. Lower collection efficiencies are also anticipated at low polymer concentrations, even if droplet size is unaffected, because the reduced amount of solids within a droplet forms a smaller particle. Since viscosity is affected by both concentration and molecular mass, lower concentrations combined with lower molecular masses may strongly and adversely influence collection efficiency.

4.2. Selecting candidate wavelengths for quantitative analysis

When constructing a calibration model from pure polymer spectra for use in predicting the composition of polymer blends and copolymers, the absorbance band intensities must be shown to be insensitive to the presence of multiple components and sensitive only to polymer amount. Fig. 3 shows a plot of the ratio of the peak area from the second derivative spectrum at 537 cm^{-1} to that at 1599 cm^{-1} for three types of samples: pure polystyrene, a 50:50 PS/PMMA blend, and a 75:25 PS/PMMA blend. Fig. 3 also shows the same type of plot for the wavelengths 699 cm^{-1} and 3026 cm^{-1}. Despite the speculation of other researchers [12], at least for the current system, no differences are evident between the various samples although precision is evidently worse at elution times corresponding to the tails of the chromatogram where low mass provides low signal-to-noise. This demonstrates that responses at these wavelengths were unaffected by the presence of methylmethacrylate in the polymer films.

4.3. Averaging spectra

Figs. 4 and 5 show plots of residuals demonstrating the advantage of averaging of the spectra from replicate samples. In Fig. 4, nineteen polystyrene fractions were obtained from each of six replicates to provide a total of 114 spectra. The absorbance response between 501 and 582 cm^{-1} of these 114 spectra were used as input to the PLS software and resulted in an estimate of polymer mass from each spectrum across the chromatogram. The six spectra at each retention volume were then averaged and the nineteen average spectra used to build a second PLS calibration model to provide nineteen estimates of average polymer mass across the chromatogram. Inspection of Fig. 4 shows that

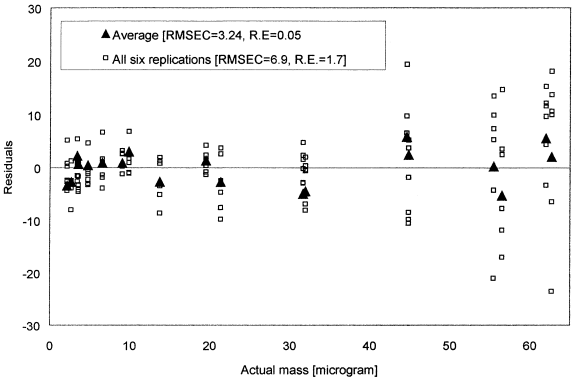

Fig. 4. Residual error in the mass of PS calculated by PLS for calibration samples of PS when individual mass values were used compared to when averages were used in application of PLS. Total calibration error (RMSEC and RE) shown in legend.

the latter values provide much lower residuals than most of the individual values.

In Fig. 5, poly(methylmethacrylate) fractions were obtained from each of three replicates to provide a total of 57 spectra. As for polystyrene, the absorbance response between 1681 and 1782 cm^{-1} of these 57 spectra were used with PLS to provide 19 estimates of the average polymer mass across the chromatogram. The three spectra at each retention volume were then averaged and used in PLS to provide 19 estimates of the average polymer mass. As for polystyrene, Fig. 5 shows that averaging improves results for PMMA analysis.

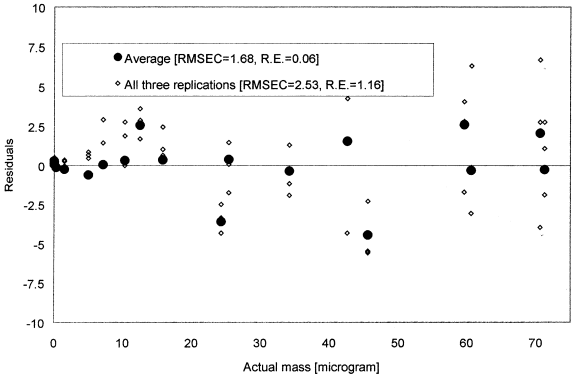

Fig. 5. Residual error in the mass of PMMA calculated by PLS for calibration samples of PMMA when individual mass values were used compared to when averages were used in application of PLS. Total calibration error (RMSEC and RE) shown in legend.

4.4. Wavelength selection based upon PLS results

With the candidate wavelengths identified and averaging shown to be the preferred method of treating the data, the next task was identifying which of the candidate wavelengths was best to employ for the PLS analysis. In our previous work [3,4], the use of multiple spectral regions showed relative errors of integrated polymer mass in the range of 3–18%. Table 2 shows RMSEC and RE values obtained for the various spectral ranges. Inspection of Table 2 as well as plots of residuals (not shown) revealed that 501–582 cm^{-1} and 1681–1782 cm^{-1} were the best regions for polystyrene and poly(methylmethacrylate), respectively, with significant reduction in error. In fact these results are superior to those obtained with narrow spectral regions using classical least squares methods [3,4].

4.5. Other data pre-processing methods

The effect of the various data pre-processing methods is shown in Table 3. Data from the 25:75 and 75:25 polystyrene–poly(methylmethacrylate) blends were used for this table. RMSEC and RE reveal that the combination of the second derivative of absorbance with respect to wavelength and mean centering provided the best values. Figs. 6 and 7 show relative error for polystyrene composition in each respective blend as calculated using various combinations of pre-processing. Results in these figures confirm the conclusion obtained from Table 3. Again the mean centering combined with second derivative was best. Relative error increased for several of the methods when elution time exceeded

Table 2
Effect of training set spectral regions

Spectral range (cm^{-1})	Component	RMSEC	R.E.
3066–2804	PMMA	2.41	1.9
1782–1681	PMMA	1.68	0.06
1639–1535	PS	4.35	1.83
1520–1378	PMMA	1.9	0.69
1056–983	PS	4.7	1.98
740–663	PS	3.68	1.13
582–501	PS	3.24	0.05

Table 3
Effect of data preprocessing using 25:75 PS/PMMA and 75:25 PS/PMMA as a calibration data set

Data preprocessing	PMMA		PS	
	RMSEC	R.E.	RMSEC	R.E.
SG2	1.9	2.58	2.44	0.5
SG2, MC	1.84	0.048	2.46	0.23
SG2, MSC	20.17	22.17	55	36.3
MC, MSC	28.96	37.4	28.99	33.57
MC, SNV	8.06	2.8	7.1	0.54
SG2, MC, MSC	70.1	115.7	56.27	100.57
SG2, MC, SNV	6.62	0.42	3.82	0.45

21 min. Polystyrene molecular mass standards were used to calculate a molecular mass scale parallel to the elution time scale in these figures. This shows that an elution time of 21 min corresponds to a polystyrene molecular mass of 200 000. In Fig. 2 we had observed a marked decrease in peak area at molecular weights below this critical value. This decreased sensitivity can be a source of scatter in Figs. 6 and 7 for elution times exceeding 21 min. Another source of scatter, present at both tails of the chromatogram, is the small mass of polymer which is present in these regions.

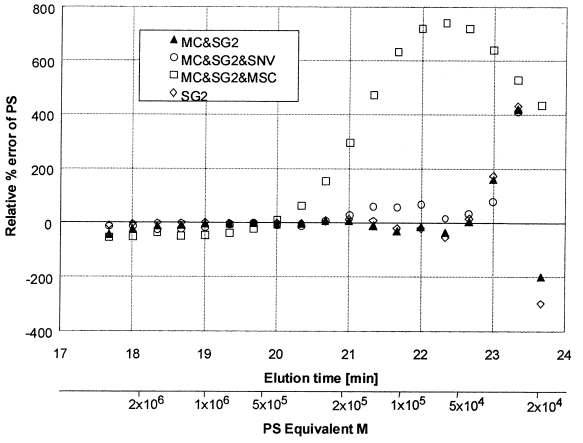

Fig. 6. Effect of data pre-processing previous to the application of PLS for the 25:75 PS/PMMA blend: RE versus retention time and polystyrene molecular mass (for comparison with Fig. 2) for four methods of data pre-processing where MC refers to mean centering, SG2 is area under the $d^2A/d\lambda^2$ at 537 cm^{-1}, SNV is standard normal variate, and MSC is multiplicative scatter correction.

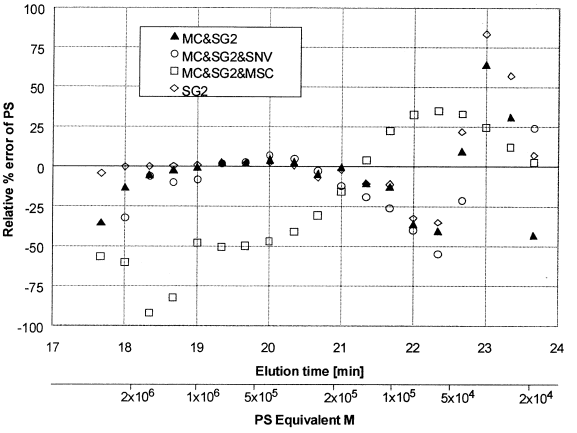

Fig. 7. Effect of data pre-processing previous to the application of PLS for the 75:25 PS/PMMA blend: RE versus retention time and polystyrene molecular mass (for comparison with Fig. 2) for four methods of data pre-processing where MC refers to mean centering, SG2 is area under the $d^2A/d\lambda^2$ at 537 cm^{-1}, SNV is standard normal variate, and MSC is multiplicative scatter correction.

4.6. Polymer blend and copolymer composition prediction

In the prediction phase of the work the results obtained from the use of only homopolymer data to calibrate PLS was contrasted with those obtained from using polymer blend data. The first objective was to see how well the known local compositions (i.e. compositions at each retention time) of a 50:50 polystyrene–poly(methylmethacrylate) blend could be predicted. Data from this blend was not used in the calibration step. The summary results in Table 4 show that total average error expressed as wt.% of a component (RMSEP) varied from 1.6 to 3.9 wt.%. Relative error, RE, (expressed as percent of the true value) ranged from 0.41 to 13.7%. Fig. 8 provides a clearer picture of the meaning of these results. There it can be seen that up to an elution time of 21.25 min predicted and DRI local compositions are very close. However, beyond 21.25 min deviations become increasingly large. As in Figs. 6 and 7, these deviations are attributed to the effect of molecular mass on detector sensitivity and at the highest times, to the difficulty in detecting the low masses present in the chromatogram low molecular mass tail. The linear dynamic range of the experiment is critically

Table 4
External validation using 50:50 PS/PMMA

Calibration	PMMA		PS	
	RMSEP	R.E.	RMSEP	R.E.
Pure PMMA and pure PS	1.91	0.41	3.9	8.56
25:75 PS/PMMA and 75:25 PS/PMMA	1.6	7.35	2.88	13.65

affected by the experimental conditions employed; for our experiments, in general >33% relative error in composition was observed when one component was present at <3 μg actual mass. Low masses may also cause scatter at the lowest times as well but such scatter is not evident in Fig. 8 because there is a significant mass of polymer at these times for this sample but it is practically all polystyrene. Results based upon the polymer blend calibration data appear marginally superior to those obtained using individual polymer component spectra. However, the small difference can be attributed to the usual observation that calibration models constructed from standards that narrowly bracket the value of an unknown provide improved results. For general composition prediction, the composition range of the unknown would have to be known in advance in order to select the correct blend samples for calibration. Therefore, PLS calibration models derived from pure polymer spectra will provide more generally satisfactory results since they encompass the entire composition range, while providing acceptable accuracy.

The second objective was to apply what we considered the best method of interpretation (PLS based upon individual homopolymer calibration) to data from styrene–methyl methacrylate copolymers. Fig. 9 shows the prediction from three replicates of weight percent methyl methacrylate (MM) monomer incorporation across the SEC chromatogram of a high-molecular-mass commercial copolymer. The SMM copolymer has a bulk average content of 30% methyl methacrylate — a value which is in accord with the range of predicted local compositions. Decreasing precision is observed in the tails of the distribution where very little copolymer was collected for FTIR analysis.

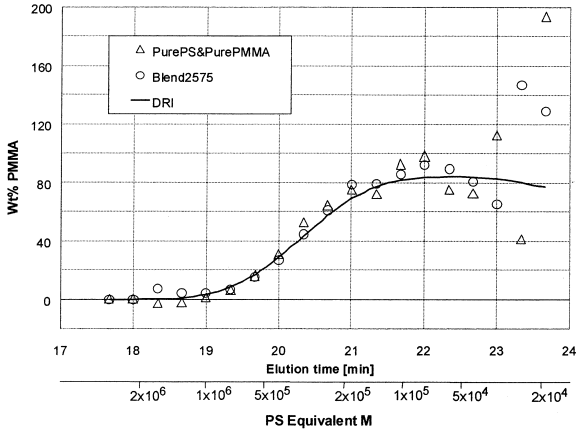

Fig. 8. Weight percent PMMA versus elution time and polystyrene molecular mass for a 50:50 PS/PMMA blend: —, the ''true'' values from the DRI chromatogram; Δ, prediction using a calibration curve from individual PS and PMMA samples; o, prediction using a calibration curve from 25:75 and 75:25 PS/PMMA blends.

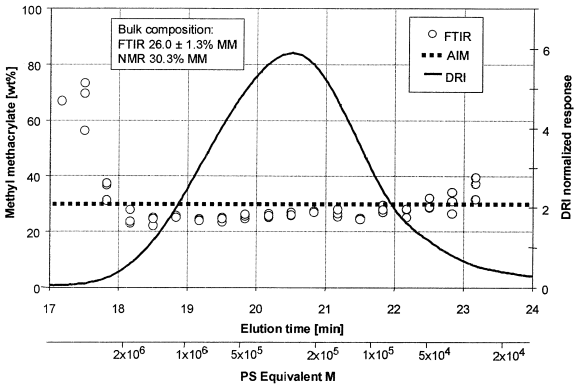

Fig. 9. Prediction of local composition for a 70:30 PS/PMMA copolymer using PS and PMMA homopolymer PLS calibration data: o, weight percent PMMA versus elution time and polystyrene molecular weight; —, DRI chromatogram; ------, average copolymer composition (from C13-NMR).

5. Conclusions

Methods of applying PLS to FTIR data obtained from annealed polymer films generated in a SEC–solvent evaporation interface were examined using styrene and methyl(methacrylate) homopolymers, blends, and copolymers. Molecular weight effects, wavelength selection, the effect of averaging spectra on results, and selection of the best data preprocessing method were investigated.

Molecular weight was found to affect FTIR absorbance data. For polystyrene it was found that below a molecular mass of 200 000 for narrow molecular mass distribution polymer standards the area under the second derivative peak ($d^2A/d\lambda^2$) at 699 cm^{-1} decreased for the same mass injected. The most probable reason for this effect was decreased efficiency of collection of polymer by the germanium disks beneath the ultrasonic nozzle. Decreased molecular mass apparently resulted in smaller droplets from the nozzle, which in turn were more easily removed by entrainment in the nitrogen flowing through the interface.

In another series of experiments, by ratioing the areas under bands at which only polystyrene was expected to absorb (537 cm^{-1} to that at 1599 cm^{-1} and at 699 cm^{-1} to that at 3026 cm^{-1}) for two different PS–PMMA blends and for polystyrene homopolymer alone, it was shown that variation in the blend composition did not significantly affect the value of the ratio. That is, the bands were considered reliable, consistent measures of polystyrene concentration in the presence of poly(methylmethacrylate).

The question of whether or not to average data previous to using it in PLS or to simply feed the software the individual data values was investigated. Pre-averaging was shown to provide values with less error than the individual values. This is consistent with the observation that variation between collected SEC runs was greater than variation within a single SEC experiment.

Screening of candidate wavelengths for polystyrene and poly(methylmethacrylate) using PLS with averaging showed that 501–582 cm^{-1} for PS and 1681–1782 cm^{-1} for PMMA provided the best fit of the calibration data. Various data pre-processing methods were then examined. It was concluded that the combination of the second derivative of absorbance with respect to wavelength and mean centering provided the best results. Throughout the paper, accuracy decreased at retention times exceeding about 21 min, the retention time corresponding to a molecular mass of 200 000. However, at extreme retention times at either end of the chromatograms, the main source of error was considered to be the very low masses of polymer present in the tails of the distribution. These low masses result in poorer quality films and low collection efficiencies due to entrainment of the very small particles.

The results of the above investigation were applied to the analysis of blend data not used in the calibration. Composition values at each retention time showed excellent agreement with known values except at retention times above 21.5 min. Calibration based upon polymer blends showed slightly better accuracy than those based upon individual homopolymers. However, the latter provide a more general and reliable basis for calibration.

Application of the homopolymer PLS model to prediction of copolymer composition was shown for a high-molecular-mass copolymer. Results are in reasonable agreement with C13-NMR bulk analysis. Local composition of the copolymer across the SEC chromatogram showed good reproducibility.

References

[1] A.H. Dekmezian, T. Moroika, C.E. Camp, J. Polym. Sci. Part B Polym. Phys. 28 (1990) 1903.
[2] P. Cheung, S.T. Balke, T.C. Schunk, Polym. Mater. Sci. Eng. 69 (1993) 122.
[3] K. Torabi, S.T. Balke, T.C. Schunk, in: Proceedings of Intern. GPC Symp, Waters Corp, 1999, pp. 167–188.
[4] K. Torabi, A. Karami, S.T. Balke, T.C. Schunk, J. Chromatogr. A 910 (2001) 19.
[5] J.N. Willis, J.L. Dwyer, M.X. Liu, Int. J. Polym. Anal. Charact. 4 (1997) 21.
[6] S. Bourne, Amer. Lab. 30 (1998) 17F.
[7] T.C. Schunk, S.T. Balke, P. Cheung, J. Chromatogr., A 661 (1994) 227.
[8] P.C. Cheung, S. Hsu, M. Tempel, S.T. Balke, L. Li, T.C. Schunk, S. Sosnowski, M.A. Winnik, Int. J. Polym. Anal. Charact. 2 (1996) 271.
[9] P.C. Cheung, S.T. Balke, T.C. Schunk, Chromatographic characterization of polymers, Adv. Chem. Ser. 247 (1995) 265.
[10] P. Cheung, S.T. Balke, T.C. Schunk, T.H. Mourey, Polymer analysis and characterization V, J. Appl. Polym. Sci.: Appl. Polym. Symp. 52 (1993) 105.

[11] V. Dhenin, L.J. Rose, Polym. Prep. 41 (2000) 285.
[12] M.X. Liu, J.L. Dwyer, Appl. Spectrosc. 50 (1996) 349.
[13] J. Adrian, E. Esser, G. Hellmann, H. Pasch, Polymer 41 (2000) 2439.
[14] D.M. Haaland, E.V. Thomas, Anal. Chem. 60 (1988) 1193.
[15] P. Geladi, P. MacDougall, H. Martens, Appl. Spectrosc. 39 (1985) 491.
[16] R.J. Barnes, M.S. Dhanoa, S.J. Lister, Appl. Spectrosc. 43 (1989) 772.
[17] O.N.M. McCallion, M.J. Patel, Intern. J. Pharm. 130 (1996) 245.
[18] B. Bittner, T. Kissel, J. Microencap. 16 (1999) 325.